

Angular dependence of spin-wave resonances and surface spin pinning in ferromagnetic (Ga,Mn)As films

X. Liu,* Y. Y. Zhou, and J. K. Furdyna

Department of Physics, University of Notre Dame, Notre Dame, Indiana 46556, USA

(Received 22 December 2006; revised manuscript received 6 March 2007; published 31 May 2007)

We present a study of exchange-dominated surface and bulk spin-wave modes in (Ga,Mn)As films grown by molecular beam epitaxy. Multimode spin-wave spectra were observed using the ferromagnetic resonance technique, as the direction of the magnetic field \mathbf{H} was varied within the plane of the layer, as well as relative to the plane. The field corresponding to the main (strongest) resonance peak at each angle is used to calculate bulk magnetic anisotropy parameters and the g factor of the magnetic films. The dependence of spin-wave (SW) modes on the orientation of \mathbf{H} is analyzed in terms of two fundamental models: the surface inhomogeneity model and the volume inhomogeneity model. Typically, when \mathbf{H} is normal or near normal to the sample plane (i.e., $\mathbf{H} \parallel [001]$), a spectrum consisting of a series of well-resolved SW modes is observed. However, as \mathbf{H} is rotated significantly away from the normal, at some orientation, a “critical angle” is found, at which only the single uniform mode is observed. As \mathbf{H} is rotated further and approaches the in-plane direction (such as the $[110]$ direction), a multiple-mode spectrum reemerges, ascribed in part to the appearance of a surface spin excitation due to unpinned surface spins. The analysis of spin-wave resonance spectra in terms of the dynamic surface spin pinning (derived from the surface anisotropy) allows us to determine the value of the exchange stiffness constant D .

DOI: 10.1103/PhysRevB.75.195220

PACS number(s): 75.50.Pp, 76.50.+g, 75.70.-i, 75.30.Ds

I. INTRODUCTION

Ferromagnetic III-Mn-V semiconductors such as (Ga,Mn)As continue to hold the interest of the scientific community, both for their fundamental scientific interest and for their potential for spintronic applications.^{1,2} Although it is well established that the ferromagnetic ordering of Mn ions in (Ga,Mn)As is induced by holes arising from the presence of Mn ions,^{3,4} our understanding of the fundamental dynamic magnetic excitations in this material—which is intimately connected with the exchange interaction between the Mn ions and the holes—is still far from complete.^{5,6} Recently, extensive studies of the magnetization dynamics in (Ga,Mn)As film have been carried out by various experimental techniques, such as the ultrafast magneto-optical Kerr effect (MOKE),^{7–10} Brillouin light scattering (BLS),¹¹ and ferromagnetic resonance (FMR).^{5,12} In this paper, we describe experiments using the FMR technique¹³ to study spin waves (the fundamental dynamic magnetic excitations in a ferromagnet) in (Ga,Mn)As films. In addition to providing considerable insight into the properties of bulk and surface magnetic excitations in (Ga,Mn)As, this method has allowed us to determine the exchange stiffness constant and the characteristics of surface spin pinning in this spin system.

The spin dynamics in ferromagnet can be described using the Landau-Lifshitz-Gilbert equation as follows:^{14–16}

$$\frac{\partial \mathbf{M}}{\partial t} = -\gamma \mathbf{M} \times \mathbf{H}_{\text{eff}} + \frac{\alpha}{M} \mathbf{M} \times \frac{\partial \mathbf{M}}{\partial t}, \quad (1)$$

where γ is the gyromagnetic constant, \mathbf{M} is the magnetization, \mathbf{H}_{eff} is the effective magnetic field within the specimen, and α is the phenomenological damping parameter. In this equation, the first and second terms represent the precessional motion and the energy dissipation, respectively. Note that the effective field \mathbf{H}_{eff} consists of a superposition of the

external magnetic field and contributions from anisotropy and exchange fields. In particular, \mathbf{H}_{eff} in a system with only uniaxial anisotropy can be described as¹⁷

$$\mathbf{H}_{\text{eff}} = -\nabla^2 \Phi + \frac{D}{g\mu_B M} \nabla^2 \mathbf{M} + \frac{2K_2}{M^2} (\mathbf{M} \cdot \mathbf{e}) \mathbf{e} + \mathbf{H}, \quad (2)$$

where $-\nabla^2 \Phi = 4\pi \nabla \cdot \mathbf{M}$ is the dipolar force, D is the exchange stiffness constant, K_2 is the uniaxial anisotropy constant, \mathbf{e} is the unit vector in the uniaxial direction, and \mathbf{H} is the external magnetic field. It can be shown from Eqs. (1) and (2) that the local magnetic anisotropy, short-range exchange interactions, and long-range dipolar forces compete in determining the static and dynamic properties of magnetic materials.

Along with previous FMR investigations carried out with the objective to understand magnetic anisotropy in (Ga,Mn)As films,^{13,18} multimode spin-wave resonance (SWR) spectra have also been observed in samples with thicknesses of 100, 150, 200, and 330 nm.^{19,20} To date, however, only SWR spectra observed in the perpendicular condition—i.e., with the dc magnetic field \mathbf{H} normal to the sample plane ($\mathbf{H} \parallel [001]$)—have been discussed for (Ga,Mn)As films, using the assumption that there exists an *asymmetric* uniaxial anisotropy profile along the growth direction.^{19,21} In this paper we report a systematic investigation of the angular dependence of SWR spectra in ferromagnetic (Ga,Mn)As films with thicknesses ranging from 100 to 200 nm. Our specific objectives are the identification of various SWR modes, exploration of surface anisotropy, and determination of the value of the exchange stiffness constant from these resonance modes. Note that, since the magnetization in ferromagnetic (Ga,Mn)As is so small that the dipole-dipole interaction in Eq. (2) can be neglected, the SW modes observed in this material are induced entirely by exchange interac-

tions. In this regard, the SW modes critically depend on some form of magnetic inhomogeneities (e.g., on the presence of a magnetization gradient or other magnetic variation along the growth direction). Such nonuniformities can either exist at the surfaces of the film (where they will be decisive in determining surface anisotropy and spin pinning conditions) or they can exist throughout the bulk of the film. In our discussion of SWR modes, we will consider such magnetic nonuniformities in terms of two fundamental models: the surface inhomogeneity (SI) model²² and the volume inhomogeneity (VI) model,²³ as discussed in the paper.

II. SAMPLE FABRICATION AND EXPERIMENTAL SETUP

The (Ga,Mn)As samples for this study were grown on (001) semi-insulating “epiready” GaAs substrates in a Riber 32 R&D molecular-beam epitaxy (MBE) system. Standard effusion cells supplied the Ga and Mn fluxes, and the flux of As₂ was produced by a cracker cell. The procedure for MBE growth of the (Ga,Mn)As/GaAs samples was as follows. First a GaAs buffer of thickness 100 nm was grown at a high substrate temperature (~ 590 °C). After cooling the substrate to 250 °C for low-temperature (LT) growth, a 2-nm-thick buffer layer of LT GaAs was grown, followed by (Ga,Mn)As layers with thicknesses ranging from 100 to 200 nm. After removing from the MBE chamber, the samples were annealed in N₂ gas for 1 h at 280 °C in order to improve materials quality both by increasing the Curie temperature and by “smoothing out” local fluctuation of composition. Unless specified otherwise, all specimens studied in this work were treated by such low-temperature annealing.

FMR measurements were carried out at 9.46 GHz using a Bruker electron paramagnetic resonance (EPR) spectrometer. In this spectrometer the applied dc magnetic field \mathbf{H} was in the horizontal plane and the microwave magnetic field was vertical. The sample was placed in a suprasil tube inserted in a liquid-helium continuous-flow cryostat, which could achieve temperatures down to 4.0 K. The experimental setup and the polar coordinate system used in the subsequent discussion are plotted in Fig. 1(a). A detailed description of the apparatus used in this investigation can be found in Ref. 13.

In this article we will focus on multimode SWR spectra and their dependence on the orientation of the dc magnetic field \mathbf{H} in two geometries, which we will refer to as the out-of-plane and in-plane geometries, as shown in Figs. 1(b) and 1(c), respectively. In the out-of-plane geometry, the (Ga,Mn)As layer was cemented to a parallelepiped of GaAs (100) substrate material, with the [110] edge of the specimen oriented vertically. Since the magnetic field \mathbf{H} of the EPR spectrometer is confined to the horizontal plane, this allowed measurements with \mathbf{H} in any intermediate orientation between the normal to the layer plane, $\mathbf{H} \parallel [001]$, and the in-plane orientation $\mathbf{H} \parallel [1\bar{1}0]$. In the in-plane geometry the sample was mounted with the layer plane horizontal (i.e., the [001] direction pointing up). In this configuration we could measure the angular dependence of the SWR spectrum when the field \mathbf{H} was confined to the (001) plane.

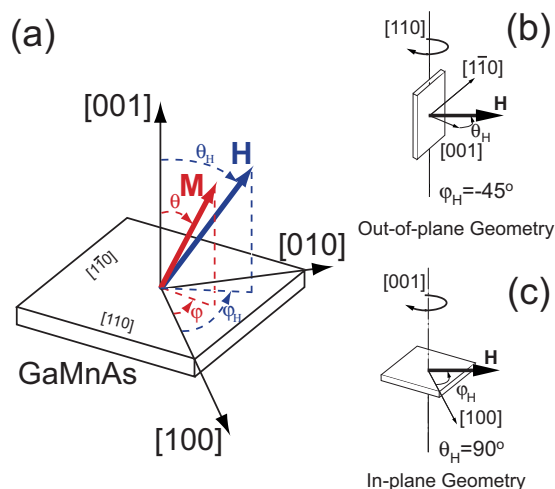


FIG. 1. (Color online) (a) Coordinate system used to describe sample configuration. The orientation of the applied dc magnetic field \mathbf{H} is described by (θ_H, φ_H) . The resulting equilibrium orientation of the magnetization \mathbf{M} is given by (θ, φ) . (b) and (c) Two experimental geometries used in this paper.

III. EXPERIMENTAL RESULTS

A. Angular dependence of spin-wave resonances

The SWR spectra observed on our samples (with thicknesses in the range from 100 to 200 nm) exhibited certain *universal* features,^{12,20,24} as illustrated by the data in Figs. 2 and 3 taken at $T=4$ K on a 120-nm-thick Ga_{0.92}Mn_{0.08}As film for several magnetic field orientations.²⁵ As shown in Fig. 2, the spectrum clearly evolves as \mathbf{H} is rotated from the out-of-plane orientation ($\mathbf{H} \parallel [001]$, $\theta_H=0^\circ$) to the in-plane orientation ($\mathbf{H} \parallel [1\bar{1}0]$, $\theta_H=90^\circ$, $\varphi_H=-45^\circ$). In particular, for $\mathbf{H} \parallel [001]$ a resonance spectrum consists of four well-resolved Portis-type SWR lines separated by equal magnetic field in-

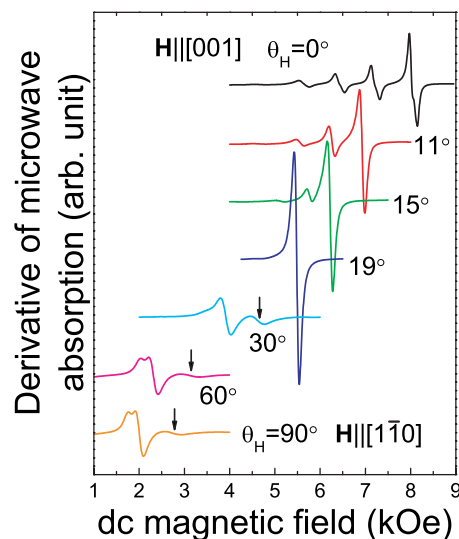


FIG. 2. (Color online) SWR spectra observed for the 120-nm Ga_{0.92}Mn_{0.08}As specimen at $T=4$ K, at various orientations θ_H for \mathbf{H} between the $[1\bar{1}0]$ and $[001]$ directions in the out-of-plane configuration ($\varphi_H=-45^\circ$). The arrows indicate the surface SW mode.

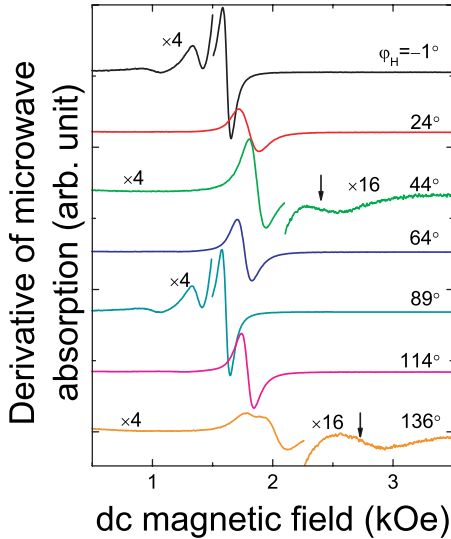


FIG. 3. (Color online) SWR spectra observed for the 120-nm $\text{Ga}_{0.92}\text{Mn}_{0.08}\text{As}$ specimen at $T=4$ K, at various orientations φ_H for \mathbf{H} in the in-plane configuration ($\theta_H=90^\circ$). The arrows indicate the surface SW mode.

crements. One should add that the number of SWR modes observed in this condition increases with increasing thickness of the film (we observe this on a series of samples with varying thickness, not shown). As one rotates \mathbf{H} away from the perpendicular orientation, the SWR modes successively disappear, and eventually—at some critical angle θ_c (19° in Fig. 2)—the multi-SW spectrum vanishes except for a single narrow resonance line. This line corresponds to the uniform FMR mode. For angle $\theta_H > \theta_c$, the multimode nature of the SW spectrum reemerges, generally containing two or three broad resonances. As demonstrated later, one of these (on the high-field side) is identified as an exchange-dominated non-propagating surface mode²² (also known as a surface spin excitation mode observed in the case of the unpinned surface spins).²⁶ Note that the complex behavior of angular dependence of the SWR spectrum described above shows some similarities to those previously observed in Permalloy and other ferromagnetic films.^{27,28} It should be mentioned that a similar behavior has recently also been observed in half-metallic ferromagnetic $\text{Co}_2\text{Cr}_{0.6}\text{Fe}_{0.4}\text{Al}$ Heusler thin films,²⁹ which suggests that the surface spin excitation may be an important feature in these newly emerging ferromagnetic alloys.

As shown in Fig. 3, the angular dependence of the SWR spectrum in the in-plane configuration shows a clear fourfold symmetry with a slight twofold distortion, the latter most likely caused by the existence of an in-plane uniaxial anisotropy field $\mathbf{H}_{2||}$, consistently observed in (Ga,Mn)As in other experiments.³⁰ At $\varphi_H=0^\circ$ ($\mathbf{H}||[100]$ —i.e., along the easy axis) the spectrum consists of at least three SWR lines, which are found to obey the Kittel quadratic relations; i.e., the separation between these modes is proportional to n^2 (n is an integer).³¹ As \mathbf{H} is rotated away from the easy axis, the multimode character of the spectrum gradually disappears and a single resonance line is also observed at φ_c (in Fig. 3, $\varphi_c=\pm 24^\circ$). As \mathbf{H} continues to approach the hard axis (the

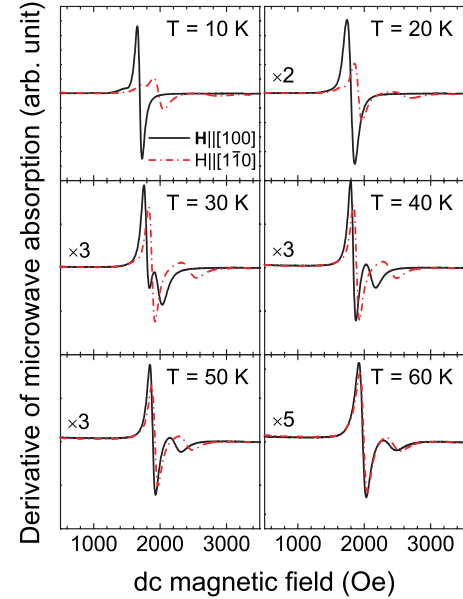


FIG. 4. (Color online) SWR spectra observed for the 120-nm $\text{Ga}_{0.92}\text{Mn}_{0.08}\text{As}$ specimen at various temperatures, at two in-plane configurations ($\mathbf{H}||[100]$ and $\mathbf{H}||[1\bar{1}0]$).

in-plane $[110]$ direction, $\varphi_H \sim \pm 45^\circ$ in Fig. 3), the spectrum transforms to one consisting of multiple absorption lines, including one corresponding to a surface mode.

Note that as the temperature increases, the Kittel type of SW structure for $\mathbf{H}||[100]$ abruptly changes to the type of SWs observed for $\mathbf{H}||[110]$, as shown in Fig. 4. In that figure the SWR spectra observed for the 120-nm $\text{Ga}_{0.92}\text{Mn}_{0.08}\text{As}$ specimen are plotted for a series of temperatures from 10 to 60 K for two in-plane configurations: $\mathbf{H}||[100]$ and $\mathbf{H}||[1\bar{1}0]$. For the configuration $\mathbf{H}||[100]$, as the temperature increases, we observe a similar evolution as that shown in Fig. 3. At 10 K the Kittel-type bulk spin-wave modes become much weaker and only a single uniform mode is observed at 20 K. Eventually, a two-mode SWR spectrum appears at higher temperatures (≥ 30 K). It is interesting that, as the bulk cubic anisotropy (which is represented by the difference between the main mode positions for the two configurations $\mathbf{H}||[100]$ and $\mathbf{H}||[1\bar{1}0]$) disappears at 60 K, the SWR full spectra for both configurations become identical. The temperature dependences of SWR spectra for $\mathbf{H}||[100]$ and $\mathbf{H}||[1\bar{1}0]$ therefore suggest that surface anisotropy, which is tightly linked to the cubic anisotropy, plays an important role in spin excitations occurring in the in-plane geometry.

The angular dependences of the mode positions are shown in Fig. 5 for the out-of-plane geometry and in Fig. 6 for the in-plane geometry. Following the convention used by Kittel,³¹ we label the successive SWR modes by odd integers $n=1,3,5,\dots$, starting from the high-field mode [where we assume *symmetric* boundary conditions for the (Ga,Mn)As film]. Since the intensity of SWRs decreases rapidly with increasing wave vector k , the main (i.e., the strongest) mode is believed to have a small k and can thus be assumed to lie very close to the theoretical field position of the uniform

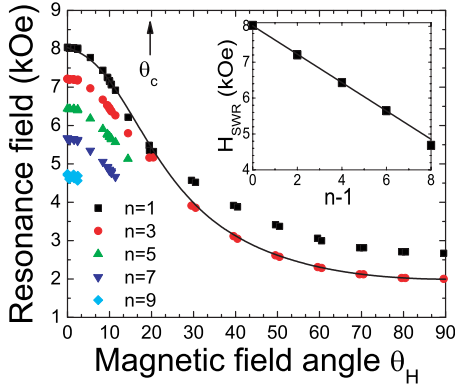


FIG. 5. (Color online) Resonant fields H_n of the SWR modes ($n=1-9$) as a function of the dc magnetic field orientation for the out-of-plane configuration. Inset: dependence of H_n measured for $\mathbf{H} \parallel [001]$ ($\theta_H=0^\circ$) on the corresponding mode number $n-1$. The line in the inset is a linear fit.

mode. In earlier analyses, its angular dependence has therefore been treated simply as a uniform mode model in determining the bulk magnetic anisotropy parameters of the thin (Ga,Mn)As films.¹³ We find that this assumption is consistent with experimental results, as discussed later. The fitting results of the present SWR data in Figs. 5 and 6 are shown as solid curves. The five bulk parameters obtained for this sample are

$$4\pi M_{eff} = 4\pi M - H_{2\perp} = 4588 \pm 34 \text{ Oe},$$

$$H_{4\perp} = 0 \pm 38 \text{ Oe},$$

$$H_{4\parallel} = 197 \pm 33 \text{ Oe},$$

$$H_{2\parallel} = 77 \pm 31 \text{ Oe},$$

$$g = 1.98 \pm 0.01.$$

Here $H_{2\perp}$ and $H_{4\perp}$ represent the perpendicular uniaxial and cubic anisotropy fields, $H_{2\parallel}$ and $H_{4\parallel}$ are the in-plane uniaxial

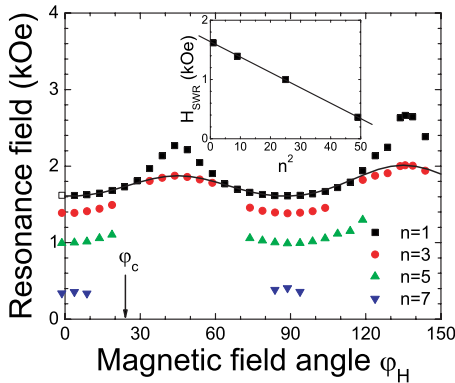


FIG. 6. (Color online) Resonant fields H_n of the SWR modes ($n=1-7$) as a function of the dc magnetic field orientation for the in-plane configuration. Inset: dependence of H_n measured at $\mathbf{H} \parallel [100]$ ($\varphi_H=0^\circ$) on the square of the corresponding mode number, n^2 . The line in the inset is a linear fit.

and cubic anisotropy fields, $4\pi M$ is the demagnetization field, and g is the spectroscopic-splitting factor.

B. Boundary conditions for spin-wave resonance

As is clearly seen from the theoretical curves in Figs. 5 and 6, the angular dependences of the SWR modes reveal two different types of SW behavior: (i) around the configuration of $\mathbf{H} \parallel [100]$ ($\varphi_H \sim 0^\circ$ and $\varphi_H \sim 90^\circ$ in Fig. 6) and $\mathbf{H} \parallel [001]$ ($\theta_H \sim 0^\circ$ in Fig. 5), the SWR spectrum consists of a main resonance line located at the highest field, with a series of weaker satellite peaks at lower fields; (ii) in contrast, around the configuration of $\mathbf{H} \parallel [110]$ or $\mathbf{H} \parallel [1\bar{1}0]$ ($\theta_H \sim 90^\circ$ in Fig. 5 and $\varphi_H \sim 45^\circ$ and $\varphi_H \sim 135^\circ$ in Fig. 6), the main resonance line is located at the lower field, below a weak peak.

The analysis of the first kind of SW structures at $\mathbf{H} \parallel [100]$ and $\mathbf{H} \parallel [001]$ shows that two different boundary conditions (corresponding to two different types of magnetic inhomogeneity) exist for these two configurations. In particular, as shown by the inset in Fig. 6, the positions of SWR modes for $\mathbf{H} \parallel [100]$ are characterized by a mode separation that varies quadratically with n . This implies that the spin precession of the SWs at the surfaces is frozen (i.e., the surface spins are tightly pinned). This represents the so-called Kittel boundary conditions, in which the position of the n th SWR mode is given by the Kittel relation³¹

$$H_n = H_0 - n^2 \frac{D}{g\mu_B} \frac{\pi^2}{L^2}, \quad (3)$$

where H_0 is the position of the theoretical uniform mode, μ_B is the Bohr magneton, n is an odd integer, and L is the sample thickness. The exchange stiffness constant D (which gives a measure of the strength of exchange interaction that tries to keep magnetic moments parallel) can then be determined from a linear fit shown in the inset in Fig. 6: $D = 43.4 \text{ meV \AA}^2$, which can also be expressed as $D/g\mu_B = 3.79 \text{ T nm}^2$.

On the other hand, as shown in the inset in Fig. 5, for $\mathbf{H} \parallel [001]$ the positions of SWR modes vary linearly with $n-1=0, 2, 4, \dots$ (our use of resonance indices is chosen so as to remain consistent with the integer sequence used by Portis in Ref. 23). This feature has been discussed previously, and the magnetic inhomogeneity required for this type of modes is assumed to originate from a nonuniform $4\pi M_{eff}$ within the film.^{19,21} Specifically, in this paper we assume a *symmetrical* parabolic $4\pi M_{eff}$ along the growth direction z ($-L/2 \leq z \leq L/2$),

$$4\pi M_{eff}(z) = 4\pi M_{eff}^0 (1 - 4\varepsilon z^2/L^2), \quad (4)$$

where ε is the ‘‘distortion parameter’’ of the film, used to define the profile of magnetic anisotropy along z . The n th (n is an odd integer) SWR mode then occurs at^{20,23,24}

$$H_n = H_0 - \left(n - \frac{1}{2}\right) (4/L) \left(4\pi M_{eff}^0 \varepsilon \frac{D}{g\mu_B}\right)^{1/2}. \quad (5)$$

If we assume that D does not depend on the orientation of \mathbf{M} , from Eq. (5) and the linear fit in the inset in Fig. 5 we

obtain $\varepsilon=0.8$. This value of ε is consistent with the field separation between the highest and lowest SWR modes observed for $\mathbf{H}\parallel[001]$ (i.e., as $H_1=8120$ Oe and $H_9=4763$ Oe, $\Delta H_{1,9}/4\pi M_{eff}=0.73$). It is interesting that the value of ε obtained above suggests the disappearance of the perpendicular uniaxial anisotropy field $H_{2\perp}$ ($\sim -4\pi M_{eff}$) at the surfaces of the film: $4\pi M_{eff}(z=\pm L/2)=0.2\times 4\pi M_{eff}^0$. This feature of $H_{2\perp}$ is also found in other (Ga,Mn)As samples studied by us with sample thicknesses between 100 nm and 200 nm.^{12,20}

As \mathbf{H} tilts away from the perpendicular direction in the out-of-plane geometry, the SW spectrum retains its linear separation but the higher-index modes gradually disappear. Eventually only a single FMR mode remains at the critical angle θ_c . This feature can *in principle* be explained by a complex mathematical approach proposed by Han based on the VI model.³² However, the value of θ_c (52°) calculated using that approach is much larger than the value of θ_c observed in our experiments (19°). Thus we can say that the VI model is quite successful in near-normal configurations, but fails at more oblique angles θ_H . This immediately implies that a more comprehensive theoretical model will be needed for interpreting the SW spectrum observed at the $\mathbf{H}\parallel[110]$ and $\mathbf{H}\parallel[1\bar{1}0]$ orientations.

C. Spin pinning at film surfaces

In 1970, Puzskarski pointed out that at surfaces of a ferromagnetic film there exists a surface anisotropy field which allows the excitation of an exchange-dominated nonpropagating surface mode and that there will be a critical orientation where only a single uniform FMR mode is observed.²² In Puzskarski's SI model^{22,23} the spin pinning condition at each film surface can be described by an effective parameter

$$A^* = 1 - (g\mu_B/2S\zeta J)(\mathbf{K}_{surf} \cdot \mathbf{m}), \quad (6)$$

where S is the atom (in our case Mn) spin, J is the Heisenberg exchange interaction parameter between two nearest spins, ζ is the number of nearest-neighbor spins in a crystal lattice, \mathbf{K}_{surf} is the effective surface anisotropy field, and \mathbf{m} is the unit vector parallel to the magnetization \mathbf{M} . Physically, parameter A^* is a measure of the pinning strength of the surface spins at the surface.

The SWR spectra and their angular dependence shown in Figs. 2, 3, 5, and 6 can be qualitatively explained by Puzskarski's SI model. In particular, when $A^* < 1$, surface spins are *pinned* and a series of bulk SWR modes with real values of the wave vectors k is observed. For $\mathbf{H}\parallel[100]$ these modes conform to the quadratic law (Kittel model), and for $\mathbf{H}\parallel[001]$ they are distorted to obey the linear law (Portis model). As \mathbf{H} tilts away from either the $[001]$ or $[100]$ direction, A^* increases, so that the surface spin pinning fades away. At the critical-angle orientation corresponding to $A^* = 1$ (e.g., $\theta_H = \theta_c = 19^\circ$, $\varphi_H = \pm 45^\circ$ or $\theta_H = 90^\circ$, $\varphi_H = \varphi_c = \pm 24^\circ$),²² only one resonance peak, corresponding to the uniform mode with $k=0$, remains. This situation corresponds to the disappearance of surface anisotropy, a case which Puzskarski has called as a "natural surface defect." When \mathbf{H} continues to approach the $[110]$ or $[1\bar{1}0]$ direction,

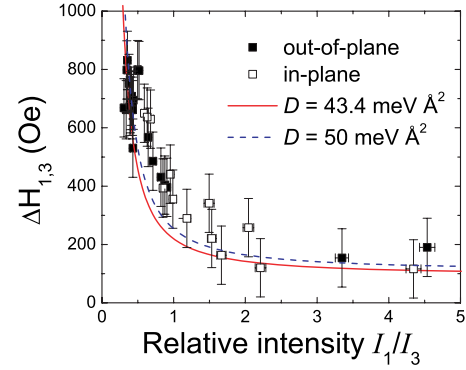


FIG. 7. (Color online) Magnetic field separation $\Delta H_{1,3}$ between the two first SW modes plotted against their relative intensity I_1/I_3 for SWR spectra where the surface modes are observed. The red solid curve is calculated based on Puzskarski's SI model using $D = 43.4$ meV \AA^2 , and the blue dashed curve is the best fit obtained with $D = 50$ meV \AA^2 .

the weak higher-field mode observed several hundred oersteds above the strongest mode, seen in Figs. 2 and 3, can be identified as a nonpropagating surface mode (i.e., k is imaginary for that mode), consistent with the case $A^* > 1$. At this condition the surface spins are *unpinned*. Note that the identification of a surface mode in the SWR spectrum is based on the following experimental facts: (a) the resonance field of the mode is above the theoretical uniform-mode position, (b) a critical-angle orientation is observed at a specific θ_c , and (c) the intensity ratio of the first two modes ($n=1$ and $n=3$) I_1/I_3 , the field separation between these two modes $\Delta H_{1,3}$, and the relation between I_1/I_3 and $\Delta H_{1,3}$ are consistent with the predictions of the SI model. As shown in Fig. 7, the relation between $\Delta H_{1,3}$ and I_1/I_3 is in remarkably good agreement with the calculated solid curve derived from Puzskarski's SI model using $D = 43.4$ meV \AA^2 , thus confirming the above identification of the mode in question as a surface SW mode. Moreover, one can thus use the relation between I_1/I_3 and $\Delta H_{1,3}$ to directly obtain the value of D by a non-linear least-squares fit. In Fig. 7 we have plotted the best fit as a blue dashed curve, which yields a consistent value $D = 50 \pm 14$ meV \AA^2 . Importantly, since the Kittel-type modes are not often observed in (Ga,Mn)As films and it is difficult to accurately determine the distortion parameter ε , the above method constitutes a reliable approach for obtaining the value of D in this material.

For completeness, the shapes (spin precession intensity as a function of z) of symmetric spin-wave modes corresponding to indices $n=1$ and 3 are shown in Fig. 8 for four specific field orientations. Comparing with the Kittel-type SW profile observed for $\mathbf{H}\parallel[100]$, the SW configuration for $\mathbf{H}\parallel[001]$ is distorted and condensed in the center of the film. In contrast to both these cases, for $\mathbf{H}\parallel[110]$ (in-plane hard axis) the SW with $n=1$ is localized at the surfaces of the film, thus forming a surface mode. At the critical angle θ_c , the parameter A^* equals 1 and only the uniform mode is observed (represented by the straight line, $k=0$, for $n=1$ in Fig. 8). The intensities of the higher modes are zero in this case.²²

We can now examine the angular dependence of surface-spin pinning conditions in more detail. Based on Puzskarski's

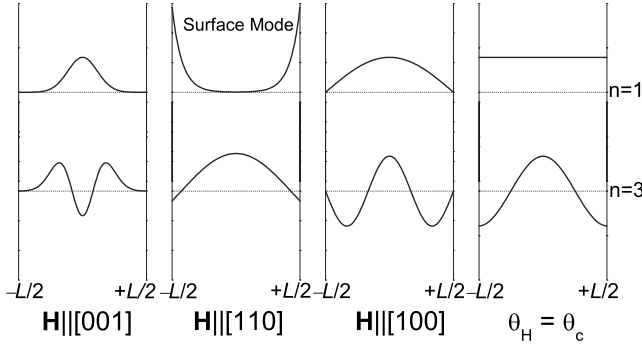


FIG. 8. Shape of the symmetric SW modes ($n=1,3$) for four specific orientations of \mathbf{H} .

ki's SI model,^{22,33} the value of A^* can be derived from the field separation $\Delta H_{1,3}$. In Fig. 9, the calculated value of A^* is plotted as a function of the magnetic field orientation both for the out-of-plane geometry (upper panel) and for in-plane geometry (lower panel). Obviously, the value of A^* is larger than 1 for $\mathbf{H} \parallel [1\bar{1}0]$ and $\mathbf{H} \parallel [110]$ ($\theta_H \sim 90^\circ$, upper panel; $\varphi_H \sim 45^\circ$ and $\varphi_H \sim 135^\circ$, lower panel), but rapidly decreases below 1 as \mathbf{H} approaches either the $[001]$ or $[100]$ direction ($\theta_H \sim 0^\circ$, upper panel; $\varphi_H \sim 0^\circ$ and $\varphi_H \sim 90^\circ$, lower panel). It should be noted that the value of A^* does not monotonically increase with increasing θ_H in the out-of-plane configuration and exhibits the expected fourfold symmetry in the in-plane configuration.

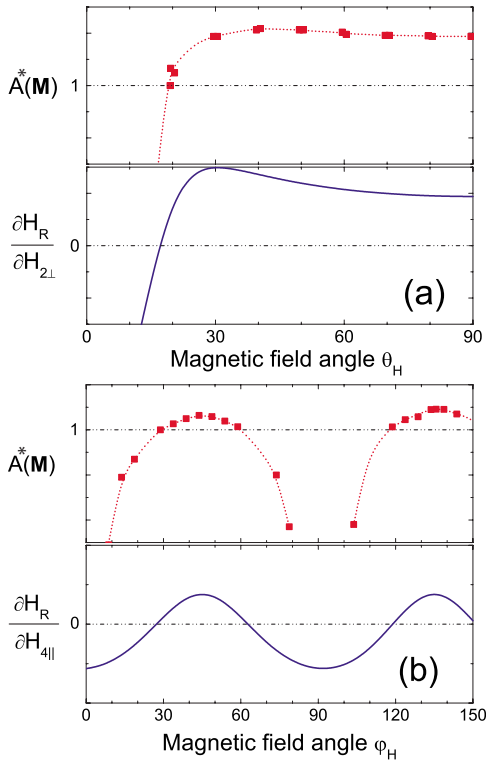


FIG. 9. (Color online) Calculated angular dependences of the surface spin pinning parameter A^* (solid square) for two configurations. The red dotted curves are guides for the eyes. The solid blue curves are the angular dependences of $\partial H_R / \partial H_{2\perp}$ and $\partial H_R / \partial H_{4\parallel}$ derived from the uniform mode model.

As shown in Fig. 9, it is found that these features can be qualitatively represented by the angular dependences of $\partial H_R / \partial H_{2\perp}$ and $\partial H_R / \partial H_{4\parallel}$, where H_R is the position of the uniform mode. Note that the critical angle is coincident with the angle where either $\partial H_R / \partial H_{2\perp}$ or $\partial H_R / \partial H_{4\parallel}$ equals zero. In other words, the critical angles are very near the angles at which the resonance field becomes independent of the small change in magnetic anisotropy. As a result, the data in Fig. 9 suggest that the magnetic anisotropy fields $H_{2\perp}$ and $H_{4\parallel}$ must differ by some amount in the bulk and surface regions.³⁴ The fact that the magnetic anisotropy field is different in the surface region (i.e., that there exists a surface anisotropy field) is the essential mechanism determining surface spin pinning and thus the character of SWR spectra observed in (Ga,Mn)As film.

Finally, we should point out that Puzskarski's SI model predicts only two critical-angle orientations [see Eq. (6)]. In order to explain the observed angular dependence of the SWR spectrum, Eq. (6) should therefore be modified by introducing the surface anisotropy in a tensorial form, including both uniaxial and cubic surface anisotropy fields.³⁵ One can, alternately, use an exact calculation with general boundary conditions.³⁶ However, generalizations to both these approaches are beyond the scope of this paper.

IV. DISCUSSION

It can be shown from Eqs. (3) and (5) that the differences between the calculated uniform mode position H_0 and the strongest SW mode in SWR spectrum is insignificant (only of the order of tens of oersteds) compared to the magnitude of both the value of the resonance field and of the bulk anisotropy field. Hence, although the surface spin pinning condition plays a critical role in determining the structure of the SWR spectrum, it has little effect on the field position of the main resonance peak. This conclusion indicates that the uniform mode model used in Ref. 30 is indeed valid for establishing bulk magnetic parameters of the (Ga,Mn)As film in the thickness range between 100 and 200 nm, such as the bulk magnetic anisotropy field and the g factor.

We should note that in this paper we have only considered *symmetric* boundary conditions. This is justified since only symmetric spin-wave modes are observed in our experiments, as seen from the monotonically waning intensities of successive SWRs (from high field to low field) for $\mathbf{H} \parallel [100]$ and $\mathbf{H} \parallel [001]$. Further evidence for this comes from the consistency of the result which we obtain for the exchange stiffness constant D for all field orientations, for both out of plane and in plane, as seen in Fig. 7. The symmetry of the boundary conditions suggests that the major source of surface anisotropy comes from the abrupt step in Mn ion or in carrier (hole) concentration at the two boundaries of the (Ga,Mn)As film, rather than the oxidation on the top surface of the sample.

The pinning parameter A^* , derived from microscopic boundary conditions, implies that the spins at the boundaries of (Ga,Mn)As experience a different anisotropy field than do the bulk spins. It has been shown that this parameter is consistent with general boundary conditions used in the macro-

scopic phenomenological approach first proposed by Rado and Weertman.^{37,36} In such a general theory, one introduces a surface free energy per unit area $F_s(\theta, \varphi)$ [or a surface anisotropy constant $K_s(\theta, \varphi)$], thus making the equations of motion for surface spins different from those for the bulk spins. The interconnection between A^* and K_s can be described as $A^* = 1 - \frac{K_s}{(DM/g\mu_B d)}$, where d is the average Mn-Mn distance.²² We thus have the relations $A^* > 1, K_s < 0$; $A^* = 1, K_s = 0$; and $A^* < 1, K_s > 0$. Note that the analysis based on such a general approach for a specific field orientation yields similar results as ours.¹⁰ A comprehensive calculation for all angles using this general approach is expected to be important for a better understanding of mechanisms of surface spin pinning in (Ga,Mn)As. In this regard, the present work should be valuable for generating a valid form of $F_s(\theta, \varphi)$.

The last issue which must be discussed is that, although the pinning parameter A^* in Puszarski's SI model provides a qualitative explanation for the angular dependence of the SWR spectrum observed in (Ga,Mn)As films, an alternate model—the Portis VI model—is needed for a detailed description of the SW spectrum observed for $\mathbf{H} \parallel [001]$. One should note that Puszarski's theory is formulated in terms of the Heisenberg localized-spin model that assumes nearest-neighbor exchange interactions and a Zeeman Hamiltonian in its standard form. This theory thus only includes the exchange interaction between nearest neighbors, assuming the exchange interaction to be short range. In the case of (Ga,Mn)As, the assumption of a “short-range” interaction is not fully justified since the pd exchange between the holes and localized Mn moments cannot be treated as short range and neither can be the superexchange interaction between Mn spins. Thus the effects of the surface anisotropy are not only felt (directly) by the spins on the surface, but the bulk spins can also be affected by the surface anisotropy through *non-local* exchange interactions. In fact, the results shown in Fig. 9 suggest that the range of the exchange interaction is determined by the strength of surface spin pinning, the magnitude of surface anisotropy, and $\partial H_R / \partial H_{2\perp}$ and $\partial H_R / \partial H_{4\parallel}$.

V. CONCLUSIONS

We have presented a detailed study of the angular dependence of the SWR spectrum in MBE-grown (Ga,Mn)As

films. The SWR modes were analyzed in the framework of the SI and VI models. The observation of a quadratic (Kittel-like) dispersion relation for $\mathbf{H} \parallel [100]$ and the surface modes for $\mathbf{H} \parallel [110]$ and $\mathbf{H} \parallel [1\bar{1}0]$ provides a clear indication that the SW modes strongly depend on surface spin pinning conditions (i.e., pinned or unpinned). In the case when \mathbf{H} is perpendicular to the sample plane, the observation of a linear (Portis-like) dispersion relation suggests that the uniaxial magnetic anisotropy field $H_{2\perp}$ is in our case probably not constant along the growth direction and nearly vanishes at the surfaces of the film. And as \mathbf{H} tilts away from either the $[001]$ or the $[100]$ directions, a “critical angle” is observed, at which only a single narrow uniform mode is excited. We thus conclude that the set of SW modes observed in the present FMR experiments clearly indicates the existence of spin pinning at the film/substrate interface and at the film surface. Moreover, using a simple SI model which takes into account dynamic surface spin pinning as well as a surface anisotropy,^{14,22,36} we have been able to explain most of the features of SWR spectra observed in our (Ga,Mn)As films.

Our analysis of SWR modes also demonstrates three intercomplementary ways for obtaining the exchange stiffness constant D : (i) from the quadratic dispersion relation of the SWR spectrum observed for $\mathbf{H} \parallel [100]$; (ii) from the linear dispersion relation of the SW modes observed for $\mathbf{H} \parallel [001]$, given that the distortion parameter $\varepsilon \sim 1$; and (iii) from the relation between the field separation and the intensity ratio of the first two SW modes. One should note that we do not yet have a good understanding of the origin of the surface spin pinning, the nonuniformity of magnetic anisotropy, and their interconnection. Thus the determination of the fundamental magnetic parameters (e.g., bulk magnetic anisotropy, g factor, exchange stiffness constant, and surface spin pinning condition) obtained from the angular dependence of SWR spectra provides an important step for gaining a better picture of spin dynamics in (Ga,Mn)As films and thus of ferromagnetism in this material generally.

ACKNOWLEDGMENTS

The authors thank D. M. Wang and R. Merlin for valuable discussions. This work was supported by NSF Grant No. DMR06-03752.

*Electronic address: xliu2@nd.edu

¹A. H. MacDonald, P. Schiffer, and N. Samarth, Nat. Mater. **4**, 195 (2005).

²I. Zutic, J. Fabian, and S. Das Sarma, Rev. Mod. Phys. **76**, 323 (2004).

³T. Dietl, H. Ohno, and F. Matsukura, Phys. Rev. B **63**, 195205 (2001).

⁴T. Jungwirth, Jairo Sinova, J. Mašek, J. Kučra, and A. H. MacDonald, Rev. Mod. Phys. **78**, 809 (2006).

⁵Jairo Sinova, T. Jungwirth, X. Liu, Y. Sasaki, J. K. Furdyna, W. A. Atkinson, and A. H. MacDonald, Phys. Rev. B **69**, 085209

(2004).

⁶J. Chovan, E. G. Kavousanaki, and I. E. Perakis, Phys. Rev. Lett. **96**, 057402 (2006).

⁷A. V. Kimel, G. V. Astakhov, G. M. Schott, A. Kirilyuk, D. R. Yakovlev, G. Karczewski, W. Ossau, G. Schmidt, L. W. Molenkamp, and Th. Rasing, Phys. Rev. Lett. **92**, 237203 (2004).

⁸Y. Mitsumori, A. Oiwa, T. Slupinski, H. Maruki, Y. Kashimura, F. Minami, and H. Munekata, Phys. Rev. B **69**, 033203 (2004).

⁹D. M. Wang, Y. H. Ren, X. Liu, Y. J. Cho, J. K. Furdyna, M. Grimsditch, and R. Merlin, AIP Conf. Proc. **893**, 1175 (2007).

¹⁰D. M. Wang, Y. H. Ren, X. Liu, J. K. Furdyna, M. Grimsditch,

- and R. Merlin, arXiv:cond-mat/0609646 (unpublished).
- ¹¹E. Harley, Ph.D. dissertation, University of North Carolina at Chapel Hill, 2006.
- ¹²Y. Y. Zhou, Y. J. Cho, Z. Ge, X. Liu, M. Dobrowolska, and J. K. Furdyna, AIP Conf. Proc. **893**, 1213 (2007).
- ¹³X. Liu and J. K. Furdyna, J. Phys.: Condens. Matter **18**, R245 (2006).
- ¹⁴P. E. Wigen, Phys. Rev. **133**, A1557 (1964).
- ¹⁵A. Aspelmeier, M. Tischer, M. Farle, M. Russo, K. Baberschke, and D. Arvanitis, J. Magn. Magn. Mater. **146**, 256 (1995).
- ¹⁶B. Heinrich, *Ultrathin Magnetic Structures* (Springer, Berlin, 1994), Vols. I and II.
- ¹⁷M. Covington, T. M. Crawford, and G. J. Parker, Phys. Rev. Lett. **89**, 237202 (2002).
- ¹⁸X. Liu, W. L. Lim, M. Dobrowolska, J. K. Furdyna, and T. Wojtowicz, Phys. Rev. B **71**, 035307 (2005).
- ¹⁹S. T. B. Goennenwein, T. Graf, T. Wassner, M. S. Brandt, M. Stutzmann, J. B. Philipp, R. Gross, M. Krieger, K. Zürn, P. Ziemann, A. Koeder, S. Frank, W. Schoch, and A. Waag, Appl. Phys. Lett. **82**, 730 (2003).
- ²⁰Y. Sasaki, X. Liu, and J. K. Furdyna, J. Supercond. **16**, 41 (2003).
- ²¹T. G. Rappoport, P. Redliński, X. Liu, G. Zaránd, J. K. Furdyna, and B. Jankó, Phys. Rev. B **69**, 125213 (2004).
- ²²H. Puzskarski, Prog. Surf. Sci. **9**, 191 (1979).
- ²³A. M. Portis, Appl. Phys. Lett. **2**, 69 (1963).
- ²⁴Y. Y. Zhou, Y. J. Cho, Z. Ge, X. Liu, M. Dobrowolska, and J. K. Furdyna, IEEE Trans. Magn. (to be published).
- ²⁵We note that our angular dependence of the SWR spectrum is slightly different from the results observed by Goennenwein *et al.*, in Ref. 19. We attribute the dissimilarities to a different magnetic inhomogeneity resulting from slight differences in the growth conditions that are unavoidable when different MBE systems are used for sample fabrication.
- ²⁶P. E. Wigen, Thin Solid Films **114**, 135 (1984).
- ²⁷T. D. Rossing, J. Appl. Phys. **34**, 1133 (1963).
- ²⁸J. Gómez, A. Butera, and J. A. Barnard, Phys. Rev. B **70**, 054428 (2004).
- ²⁹B. Rameev, F. Yildiz, S. Kazan, B. Aktas, A. Gupta, L. R. Tagirov, D. Rata, D. Buergler, P. Gruenberg, C. M. Schneider, S. Kämmerer, G. Reiss, and A. Hütten, Phys. Status Solidi A **203**, 1503 (2006).
- ³⁰X. Liu, Y. Sasaki, and J. K. Furdyna, Phys. Rev. B **67**, 205204 (2003).
- ³¹C. Kittel, Phys. Rev. **110**, 1295 (1958).
- ³²Z.-Q. Han, J. Magn. Magn. Mater. **140**, 1995 (1995).
- ³³H. Puzskarski, Acta Phys. Pol. A **38**, 217 (1970); Phys. Lett. **38**, 899 (1970).
- ³⁴P. E. Wigen, C. F. Kooi, M. R. Shanabarger, and T. D. Rossing, Phys. Rev. Lett. **9**, 206 (1962).
- ³⁵J. T. Yu, R. A. Turk, and P. E. Wigen, Phys. Rev. B **11**, 420 (1975).
- ³⁶A. Maksymowicz, Phys. Rev. B **33**, 6045 (1986).
- ³⁷G. Rado and J. Weertman, J. Phys. Chem. Solids **11**, 315 (1959).